

## Techno-economic optimization of a scaled-up solar concentrator combined with CSPonD thermal energy storage

Richard Musi, Benjamin Grange, Miguel Diago, Monika Topel, Peter Armstrong, Alexander Slocum, and Nicolas Calvet

Citation: [AIP Conference Proceedings](#) **1850**, 110010 (2017); doi: 10.1063/1.4984484

View online: <https://doi.org/10.1063/1.4984484>

View Table of Contents: <http://aip.scitation.org/toc/apc/1850/1>

Published by the [American Institute of Physics](#)

---

### Articles you may be interested in

[CSPonD demonstrative project: Start-up process of a 25 kW prototype](#)

[AIP Conference Proceedings](#) **1850**, 110003 (2017); 10.1063/1.4984477

[Techno-economic analysis of concentrated solar power plants in terms of levelized cost of electricity](#)

[AIP Conference Proceedings](#) **1850**, 160018 (2017); 10.1063/1.4984552

[Start-up performance of parabolic trough concentrating solar power plants](#)

[AIP Conference Proceedings](#) **1850**, 160008 (2017); 10.1063/1.4984542

[Enhancing economic competitiveness of dish Stirling technology through production volume and localization: Case study for Morocco](#)

[AIP Conference Proceedings](#) **1850**, 050002 (2017); 10.1063/1.4984406

[Optical property characterization of molten salt mixtures for thermal modeling of volumetrically absorbing solar receiver applications](#)

[AIP Conference Proceedings](#) **1850**, 070005 (2017); 10.1063/1.4984419

[Particles fluidized bed receiver/reactor tests with quartz sand particles using a 100-kW<sub>th</sub> beam-down solar concentrating system at Miyazaki](#)

[AIP Conference Proceedings](#) **1850**, 100012 (2017); 10.1063/1.4984469

---

# Techno-Economic Optimization of a Scaled-Up Solar Concentrator Combined with CSPonD Thermal Energy Storage

Richard Musi<sup>1,2</sup>, Benjamin Grange<sup>1</sup>, Miguel Diago<sup>1</sup>, Monika Topel<sup>3</sup>,  
Peter Armstrong<sup>1</sup>, Alexander Slocum<sup>4</sup>, and Nicolas Calvet<sup>1,a)</sup>

<sup>1</sup> Institute Center for Energy (iEnergy), Department of Mechanical and Materials Engineering, Masdar Institute of Science and Technology, Masdar City, P.O. Box 54224, Abu Dhabi, United Arab Emirates.

<sup>2</sup> Université de Perpignan Via Domitia (UPVD), 52 Avenue Paul Alduy, 66860 Perpignan Cedex, France.

<sup>3</sup> Energy Department, KTH Royal Institute of Technology, SE-100 44, Stockholm, Sweden.

<sup>4</sup> Department of Mechanical Engineering, Massachusetts Institute of Technology (MIT),  
77 Massachusetts Ave, Cambridge, MA 02139, United States of America.

<sup>a)</sup> **Contact:** Dr. Nicolas Calvet, Chair of the Masdar Institute Solar Platform, Assistant Professor.  
Phone: +971 2 810 9413. E-mail: [ncalvet@masdar.ac.ae](mailto:ncalvet@masdar.ac.ae)

**Abstract.** A molten salt direct absorption receiver, *CSPonD*, used to simultaneously collect and store thermal energy is being tested by *Masdar Institute* and *MIT* in Abu Dhabi, UAE. Whilst a research-scale prototype has been combined with a beam-down tower in Abu Dhabi, the original design coupled the receiver with a hillside heliostat field. With respect to a conventional power-tower setup, a hillside solar field presents the advantages of eliminating tower costs, heat tracing equipment, and high-pressure pumps. This analysis considers the industrial viability of the *CSPonD* concept by modeling a 10 MW<sub>e</sub> up-scaled version of a molten salt direct absorption receiver combined with a hillside heliostat field. Five different slope angles are initially simulated to determine the optimum choice using a combination of lowest LCOE and highest IRR, and sensitivity analyses are carried out based on thermal energy storage duration, power output, and feed-in tariff price. Finally, multi-objective optimization is undertaken to determine a Pareto front representing optimum cases. The study indicates that a 40° slope and a combination of 14 h thermal energy storage with a 40-50 MW<sub>e</sub> power output provide the best techno-economic results. By selecting one simulated result and using a feed-in tariff of 0.25 \$/kWh, a competitive IRR of 15.01 % can be achieved.

## INTRODUCTION

A molten salt direct absorption receiver is currently being tested by *Masdar Institute* and *MIT* in Abu Dhabi, UAE. The Concentrated Solar Power on Demand Demonstration (*CSPonD Demo*) project, first proposed in 2011 [1], was initially based on a hillside heliostat field. However, the pre-commercial prototype is being tested with a beam-down tower, also called tower reflector [2], located at the Masdar Institute Solar Platform (*MISP*).

Very little research has been carried out as to the scalability and associated costing of a beam-down concentrator (either a beam-down tower or hillside heliostat field) with *CSPonD* thermal storage. Indeed, Vant-Hull argues that “beam-down system costs are difficult to obtain ... because there have been few design studies that have produced publicly available costs” [3].

The aim of this study is to design a scaled-up *CSPonD* thermal energy storage system combined with a hillside heliostat field, a representation of which is shown in Fig. 1. Such a system presents the advantages of eliminating the conventional tower-mounted receiver, heat tracing equipment to prevent heat transfer fluid (HTF) freezing and high-pressure pumps. A beam-down tower study is omitted but should be treated in a future paper to compare results.

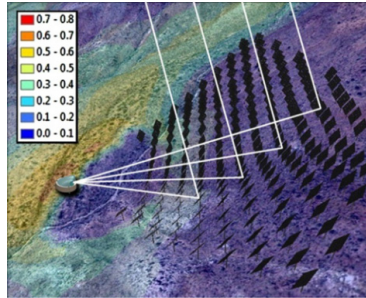


**FIGURE 1.** Representation of a hillside solar field with *CSPonD* receiver [1].

The main focus of this analysis is on optimizing system configuration based on power output, thermal energy storage (TES) and solar multiple for a given slope, whilst at the same time minimizing LCOE and initial investment.

## METHODOLOGY

The study is carried out in four main phases:

1. Obtaining CSP market and *CSPonD* benchmark cost information:
  - ⇒ Carrying out CSP market cost analyses to obtain cost per major component;
  - ⇒ Establishing total cost for the existing 100 kW<sub>th</sub> beam-down and *CSPonD Demo* system installed at the *MISP* in the UAE.
2. Developing an optical optimization model using the *MUEEN* code [4], to design an up-scaled *CSPonD* system using a hillside heliostat field for a given power output;
3. Calculating the optical efficiency of each upscaled system using *TracePro*;
4. Determining total cost and analyzing different economic indicators for the scaled-up system based on multi-objective optimisation using *DYESOPT*.

### CSP Market and *CSPonD* Benchmark Costing

CSP market costing per major component (Table 1) is determined through a combination of study analysis [5-7] and discussions with industry (notably *eSolar* [8] and *Helio 100* [9]).

**TABLE 1.** Cost assumptions per major component.

	Cost per unit (\$)
Solar Field (\$/m <sup>2</sup> )	180.34
Power Block (kW <sub>e</sub> - gross)	1039.00
O&M (\$/kW <sub>e</sub> /year)	90.20
Land Preparation & Purchase (\$/kW <sub>th</sub> )	307.96
Central Reflector (\$/kW <sub>th</sub> )	725.90
HTF (\$/kg)	1.00

Using the assumptions shown in Table 1 along with known outlay for the *CSPonD Demo* receiver, a total cost of between 24,000-27,000 \$/kW<sub>e</sub> (depending on financing conditions) for the *MISP*'s 100 kW<sub>th</sub> beam-down and 24 h *CSPonD* thermal energy storage (TES) is obtained. Given this total cost, that the heliostat field is 280.7 m<sup>2</sup> and assuming 12 % overall plant efficiency, an LCOE of between 0.443-0.508 \$/kWh is found for the prototype system. This LCOE is high compared to industrial CSP plants [10] but can be expected given the small scale and research driven aims of the prototype.

## Optical Optimization Model

Having determined base costing for a prototype sized system, the authors now focus on building an optical optimization model in order to upscale the *CSPonD* receiver with a hillside heliostat field. The main distinguishing point of this model with regard to typical power-tower plants is the need to position heliostats on a slope to simulate the hillside.

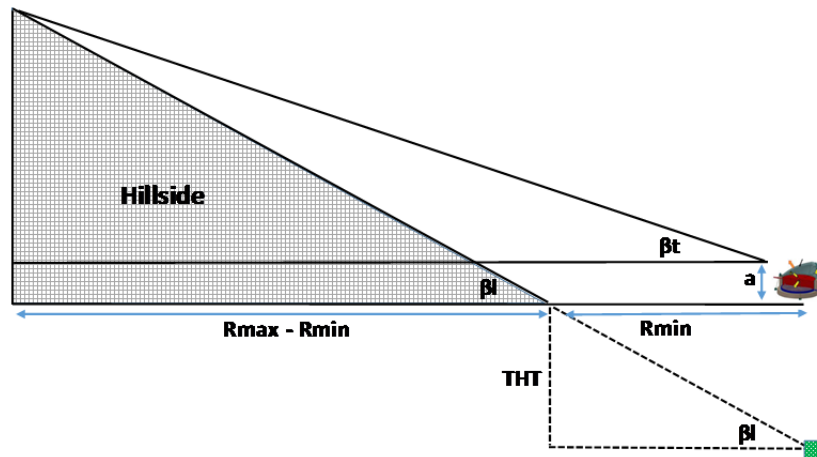
The *MUEEN* code, based on a radially-staggered layout which places heliostats so as to eliminate blocking losses over the year, is used to build the hillside field. For this study, *MUEEN* presents the advantage of incorporating the ability to modify slope angle.

Different simulations are tested (Table 2), each with a slope angle differing in increments of  $10^\circ$ , yielding five unique solar field layouts. Converting the slope angle to an average beam-down angle ( $\beta_t$ ) allows for a comparison of this study with past analysis [11].

**TABLE 2.** Characteristics of the five simulated cases.

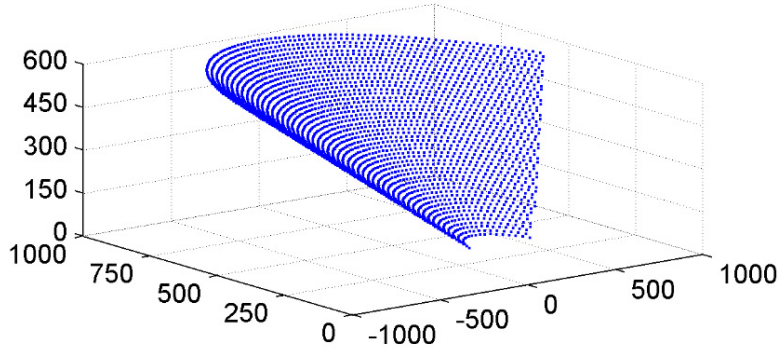
Case	1	2	3	4	5
Slope Angle ( $\beta_l$ ) ( $^\circ$ )	10	20	30	40	50
Beam-Down Angle ( $\beta_t$ ) ( $^\circ$ )	7.89	16.43	25.3	34.64	44.56
Rmin (m)	200	200	200	200	200
Tower Height (THT) (m)	35.27	72.79	115.47	167.82	238.35
Rmax (m)	1 000	1 000	1 000	1 000	1 000
Receiver height (a) (m)	10	10	10	10 </td <td>10</td>	10
Number of heliostats	2 567	2 800	2 984	3 430	4 362
Heliostat Area (m <sup>2</sup> )	205 360	224 000	238 720	274 400	348 960

Fig. 2 shows a representation of how the hillside heliostat field is inputted into *MUEEN*. As the field slope is assumed, in the code, to start from the receiver (shown by the green square), it is necessary to calculate the corresponding “tower height” (THT) that places the receiver at ground level. In this way, it is possible to simulate flat ground from the receiver for a distance of  $R_{min}$  before the hillside slope begins. Using the minimum solar field radius  $R_{min}$  along with the tangent of the slope angle  $\beta_l$  allows for the calculation of the theoretical THT for each of the five cases.



**FIGURE 2.** Representation of the hillside solar field inputted into *MUEEN*.

The resulting inputs used to create the different solar fields in *MUEEN* are shown in Table 2, where in each case the individual heliostat area is  $80 \text{ m}^2$ . An  $R_{min}$  of 200 m is chosen as a compromise between attenuation and heliostat blocking, where a smaller  $R_{min}$  would lead to increased blocking and a larger  $R_{min}$  higher attenuation. Whilst the authors assume an  $R_{min}$  value, in a future study this could be varied in order to determine optimal overall efficiency for each field slope. Figure 3 displays the field layout simulation using *MUEEN* with a  $30^\circ$  slope. Heliostat field density increases with increasing slope and decreases with increasing distance from the receiver.



**FIGURE 3.** Hillside heliostat field for a 30° slope. All dimensions are in meters.

### Optical Efficiency Calculations

The five cases are run in the ray tracing software *TracePro* 7.57 [12] to create a matrix calculating overall optical efficiency (the product of the cosine, shading, blocking and spillage efficiencies) based on differing sun elevations and azimuths.

An in-house code is written to compute efficiency based on the flux reported by *TracePro* on each surface after each simulation. The heliostats are modeled as flat, perfect mirrors oriented with an azimuth-elevation scheme, forming a south-facing field, and the receiver is simulated being placed at the z-axis of the model. The sun is represented as a large, flat circular source above the field and each ray direction is determined on the basis of the solar angular distribution included in *TracePro*.

### Multi-Objective Optimization

The overall optical efficiencies calculated by *TracePro* are then inputted into *DYESOPT*, a techno-economic modeling tool developed at *KTH Royal Institute of Technology* [13-14], with the solar field being sized for each case to account for a target power output of 10 MW<sub>e</sub> and 2-hour TES. The *CSPonD* receiver is modeled in *DYESOPT* based on the equations indicated in [11], with power transferred to the lid being ignored leading to an overestimation of losses. In general, thermal receiver losses are negatively correlated to beam-down angle. *DYESOPT* simulates annual production for each case taking into account atmospheric attenuation based on 15 km visibility [15] and 95 % heliostat reflectivity, and using typical meteorological year (TMY) data for the UAE.

For each of the five cases, total capital and operating expenditure (respectively CAPEX and OPEX) are derived by *DYESOPT* and verified with the assumptions indicated in Table 1. Finally, economic indicators such as LCOE, ROI and IRR are calculated to evaluate the different cases, with the corresponding equations and assumptions being found in [9].

## RESULTS

A techno-economic analysis is initially carried out to compare different hillside slope angles, with an optimal case being chosen. Sensitivity analysis is then undertaken on this optimal slope case to observe changes based on differing power output, thermal energy storage and feed-in tariff. Finally, a multi-objective optimization carried out in *DYESOPT* combines solar multiple, power output and thermal energy storage as input variables in order to determine optimal combinations, based on an objective of minimizing LCOE and CAPEX.

### Techno-Economic Analysis for All Slopes

Table 3 summarizes the main technical findings for each of the 5 cases, where each solar field is built in *DYESOPT* using a target power output of 10 MW<sub>e</sub>. Cells highlighted in red indicate worst performance for the given metric, those in green best performance.

**TABLE 3.** Key technical findings for the five slopes.

Slope (°)	Solar Field Aperture (m <sup>2</sup> )	Annual Production (GWh)	Solar Field Efficiency (%)	Overall Efficiency (%)	Capacity Factor (%)
10	204 800	18.58	19.93%	6.04%	25.40%
20	125 280	18.77	33.21%	10.08%	25.69%
30	101 920	18.22	39.86%	12.11%	24.97%
40	104 160	18.92	40.72%	12.40%	25.92%
50	113 600	18.37	36.33%	11.06%	25.18%

Despite having the largest solar field, a 10° slope produces the third lowest overall annual production due to a low solar field efficiency caused principally by high shading losses. The optimum field from a technical standpoint is situated on a 40° slope, which provides the highest overall annual efficiency and the highest capacity factor. Capacity factors, in general, are relatively low given that this simulation assumed 2 hours of thermal energy storage with a solar multiple of 1.5.

By factoring in the economic results displayed in Table 4 it is now possible to determine an optimum case for our simulation. Once again the red cells indicate worst performance and the green cells best performance. The 10° slope has the highest total cost mainly due to having the largest solar field, which as a component provides the highest proportional cost of current CSP plants [18]. Combined with low production as a result of low overall efficiency, the 10° slope has the lowest IRR and the highest LCOE, indicating worst overall performance.

**TABLE 4.** Key economic findings for the five slopes.

Slope (°)	Total Cost (M\$)	Payback Period (years)	NPV (M\$)	ROI (%)	IRR (%)	LCOE (\$/kWh)
10	146.36	23.22	-18.90	-29.35%	3.92%	0.279
20	100.23	15.25	3.90	9.22%	7.78%	0.189
30	89.16	13.70	7.54	20.35%	8.80%	0.173
40	88.43	13.15	10.05	27.40%	9.45%	0.166
50	90.32	13.81	7.45	19.80%	8.75%	0.174

A 40° slope has the lowest CAPEX owing to higher heliostat density and lower land use than the 30° slope, and provides the highest ROI and IRR combined with the lowest LCOE of the five cases. A commonly used hurdle rate for IRR calculations is 10 %, indicating that with the assumed feed-in tariff (0.25 \$/kWh) a plant installed on a 40° slope would be of most interest to typical investors.

### Sensitivity Analysis for the Optimum Slope

In order to observe changes based on different variables, sensitivity analysis is carried out with varying power output (10-50 MW<sub>e</sub>), TES duration (2-15 h) and feed-in tariff (0.15-0.30 \$/kWh). Modifying the FiT will not impact LCOE, so IRR will be the dependent variable in this case.

**TABLE 5.** Sensitivity analysis for a 2 h TES plant with 40° slope and varying power outputs.

Slope (°)	Net Power (MW <sub>e</sub> )	Solar Field Aperture (m <sup>2</sup> )	Total Cost (M\$)	Annual Production (GWh)	Overall Efficiency (%)	Payback Period (years)	ROI (%)	IRR (%)	LCOE (\$/kWh)
40	10.00	104 160	88.43	18.92	12.40	13.1	27.40%	9.45%	0.166
	20.00	193 920	155.74	39.88	13.26	10.9	57.79%	12.12%	0.138
	30.00	292 320	222.46	61.67	13.58	10.0	73.64%	13.47%	0.128
	40.00	377 600	282.80	80.78	13.62	9.6	79.87%	13.99%	0.124
	50.00	467 200	343.13	100.40	13.62	9.3	85.15%	14.43%	0.121

The 40° slope is chosen as the optimal case given that it provides the best combination of low LCOE and high IRR, and now forms the basis for the subsequent sensitivity analysis. The thermal receiver losses for this slope combined with 10 MW<sub>e</sub> power output and 2 h TES are calculated to be around 18.5%.

Table 5 runs sensitivity analysis on a 40° slope and 2 h TES with power output varying from 10 to 50 MW<sub>e</sub> in increments of 10 MW<sub>e</sub>. Increasing power output brings increasing IRR and reducing LCOE, indicating that a larger plant would bring better economic results which can principally be attributed to economies of scale.

**TABLE 6.** Sensitivity analysis for a 10 MW<sub>e</sub> plant with 40° slope and varying thermal energy storage (TES).

Slope (°)	TES (h)	Solar Field Aperture (m <sup>2</sup> )	Total Cost (M\$)	Annual Production (GWh)	Capacity Factor (%)	Payback Period (years)	ROI (%)	IRR (%)	LCOE (\$/kWh)
40	2	163 680	115.19	26.84	30.6%	13.1	43.67%	10.93%	0.152
	6	193 920	136.86	36.18	41.3%	12.1	67.02%	12.97%	0.134
	10	236 000	161.51	45.83	52.3%	11.6	81.20%	14.18%	0.125
	14	268 800	183.02	54.60	62.3%	11.2	91.61%	15.07%	0.119
	18	292 320	201.32	60.06	68.6%	11.4	91.71%	15.08%	0.119

In reality, the limiting factor with increasing power size for a hillside heliostat field will be land area, whereby finding a harmonious slope over a large distance will be increasingly difficult as power output and solar field size increase.

Results are similar when varying TES duration as an independent variable (Table 6), where increasing TES reduces LCOE and increases IRR, although the lowest payback period is found for 14 h TES. As for power output, having more TES will lead to a larger solar field, and as solar multiple increases the geographic constraints of the hillside will increasingly come into play.

Modifying the assumed feed-in tariff (FiT) for the plant's revenue streams influences IRR whilst leaving LCOE unchanged. Table 7 shows the impact of changing the FiT on the reference 10 MW<sub>e</sub> plant with 40° slope and 2 h TES. Implementing a 0.30 \$/kWh in line with the tariff received by the Spanish CSP plants would lead to an attractive IRR above 10 %. This IRR would interest investors, allowing the technology to demonstrate its potential on an industrial scale, with the FiT being reduced for subsequent plants as the technology matures.

**TABLE 7.** Sensitivity analysis for a 10 MW<sub>e</sub> plant with 40° slope and varying feed-in tariff (FiT).

	IRR (%) 0.15\$/kWh FIT	IRR (%) 0.20\$/kWh FIT	IRR (%) 0.25\$/kWh FIT	IRR (%) 0.30\$/kWh FIT
10MW <sub>e</sub> , 40° slope	3.05%	6.43%	9.45%	12.27%

## Multi-Objective Optimization

Having changed variables independently during the previous analysis, the authors now combine power output (10-50 MW<sub>e</sub>), thermal energy storage (2-18 h) and solar multiple (1.5-7) to carry out multi-objective optimization (MOO). Various simulations are run in *DYESOPT* with an aim of determining optimal combinations based on minimizing LCOE and CAPEX. In order to examine the tradeoffs, *DYESOPT* incorporates a modified version of *QMOO*, a multi-objective optimizer developed at the *Industrial Energy Systems Laboratory* in Lausanne [19].

Figures 4-7 display results with dependent variables being LCOE and CAPEX, where each dot represents a unique combination of the three independent variables.

By looking at how power output and solar field aperture influence results (Figs. 4-5), it can be seen that economies of scale dominate and a larger plant or solar field lead to a lower LCOE but at the same time higher CAPEX. Although the simulations found along the Pareto front represent optimal cases for a given CAPEX, there is no unique optimum, whereby an investor may choose a smaller solar field to obtain a smaller CAPEX investment, even though the LCOE may be higher.

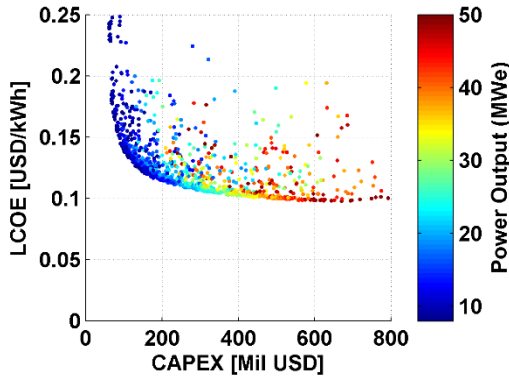


FIGURE 4. MOO focusing on power output ( $MW_e$ )

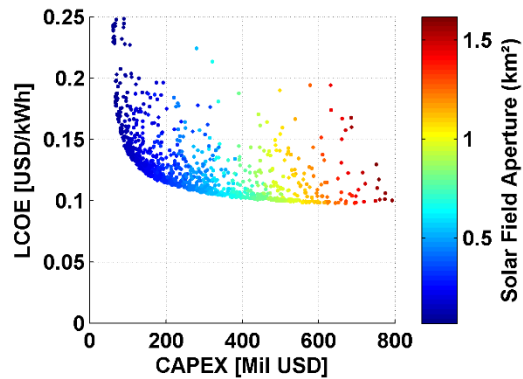


FIGURE 5. MOO focusing on solar field aperture ( $km^2$ )

Figures 6-7 show the impact of capacity factor and TES on the simulations. In these cases, higher capacity factor and increased TES dominate the Pareto front, indicating that these two variables are important elements to consider when looking to optimize such a CSP plant. Indeed, irrespective of CAPEX, the lowest LCOE can be found for a TES of approximately 14 h and a capacity factor of approximately 60 %. This result is encouraging for the CSP industry as it would allow the technology to exploit its dispatchability as a compliment to other forms of Renewable Energy.

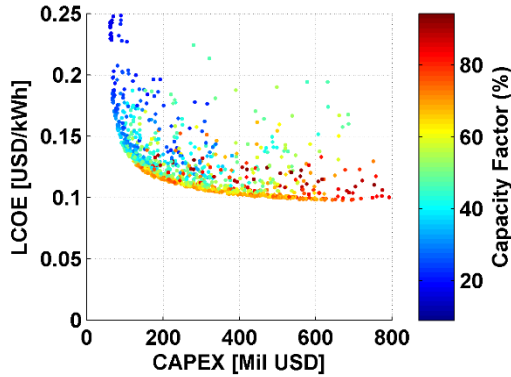


FIGURE 6. MOO focusing on capacity factor (%)

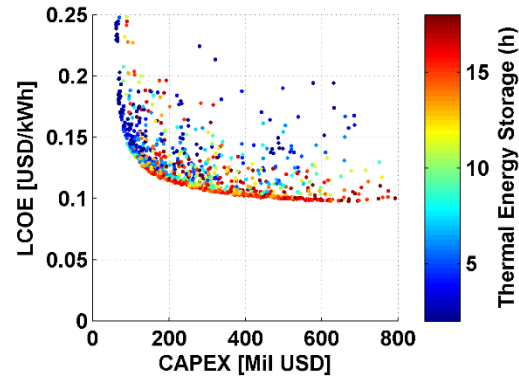


FIGURE 7. MOO focusing on thermal energy storage (h)

## CONCLUSION

This study presents a foundation analysis of an up-scaled molten salt direct absorption receiver (*CSPonD*) combined with a hillside heliostat field. Such a concept uses natural topography to place heliostats on a hillside which beam down their concentrated sunlight to a receiver at ground level, thus eliminating tower costs, heat-tracing equipment, and high-pressure pumps with respect to a conventional power tower.

This analysis has used a multi-tool approach combining *MUEEN* to build up a hillside solar field, *TracePro* to evaluate optical efficiency and *DYESOPT* to carry out multi-objective optimization. Through this study, it has been found that a  $40^\circ$  slope provides the best techno-economic results and that combining with 14 h TES provides an attractive investment opportunity. Whilst larger power outputs provide slightly reduced LCOE, CAPEX increases and additionally finding a suitable hillside without undertaking major earthwork could prove complex. This concept would thus seem most suited to a power output of 10-20  $MW_e$ , and combined with a  $40^\circ$  slope and 14 h TES, could lead to an attractive LCOE of between 0.10-0.15  $\$/kWh$ . By selecting one simulated result with 10  $MW_e$  power output, 16 h TES, a solar multiple of 4 and a feed-in tariff of 0.25  $\$/kWh$ , an IRR of 15.01 % can be achieved.

In terms of future studies, initial ways to further this analysis include varying  $R_{min}$  to see the effect on heliostat blocking and overall efficiency, refining slope increments to  $1^\circ$  around the  $30$ - $50^\circ$  range to target an improved



optimum, choosing real world case studies to see accessibility in terms of hill slope and available area, conducting a more thorough assessment of *CSPonD* losses to include power transferred to the lid, combining *MUEEN*, *TracePro* and *DYESOPT* into a single interface, and carrying out a similar analysis for a *CSPonD* receiver coupled with a beam-down tower and with a conventional flat terrain case in order to compare results.

## ACKNOWLEDGEMENTS

This work is funded by the *Masdar Institute/MIT* collaborative flagship project, grant # FR2014-000002. Research at Masdar Institute is supported by the Government of Abu Dhabi to help fulfill the vision of the late President Sheikh Zayed bin Sultan Al Nayhan for sustainable development and empowerment of the UAE and humankind.

*Masdar Institute* and *MIT* acknowledge in alphabetic order: *Dongfang Electric Corporation* for designing and providing the molten salt-air heat exchanger system, *National Instruments* and *Parker/Sunpower* for donating part of the instrumentation, control, and motion systems, and *SQM* for kindly providing the nitrate salts for the prototype.

## REFERENCES

1. A. Slocum *et al*, “Concentrated Solar Power on Demand” (2011) *Solar Energy* 85, 1519–1529
2. A. Rabl, “Tower Reflector for Solar Plants” (1976), *Solar Energy* 18, 269-271
3. L. Vant-Hull, *SolarPACES* 2013: “Issues with beam-down concepts” (2013)
4. F. M. F. Siala and M. E. Elayed, “Mathematical formulation of a graphical method for a no-blocking heliostat field layout” (2000)
5. C. Turchi *et al*, “Current and Future Costs for Parabolic Trough and Power Tower Systems in the US Market” (2010)
6. US DOE’s Sunshot research: <http://energy.gov/eere/sunshot/csp-component-research-and-development>
7. W. Vogel and H. Kalb, “Large Scale Thermal Power” (2010)
8. R. Huibregtse from eSolar: <http://www.esolar.com/> (private communication)
9. W. Landman from Helio 100: <http://helio100.sun.ac.za/> (private communication)
10. R. Musi *et al*, “Techno-Economic Analysis of Concentrated Solar Power Plants in terms of Levelized Cost of Electricity” (2016) Proceedings of the International *SolarPACES* Conference 2016. Abu Dhabi, UAE. October 11-14, 2016.
11. D. Codd and A. Slocum, “Direct Absorption Volumetric Molten Salt Receiver with Integral Storage” (2011) *ASME* 2011 5th International Conference on Energy Sustainability, Paper No. ES2011-54175, pp. 511-521
12. *TracePro* <http://www.lambdare.com/tracepro>
13. J. Spelling, “Hybrid solar gas-turbine power plants: A thermo-economic analysis” Ph.D. thesis, KTH Royal Institute of Technology, 2013.
14. R. Guédez, M. Topel, J. Spelling and B. Laumert, “Enhancing the profitability of solar tower power plants through thermo-economic analysis based on multi-objective optimization” in International Conference on Concentrating Solar Power and Chemical Energy Systems, *SolarPACES* 2014 (Energy Procedia), pp. 1277-1286.
15. B. Kistler, “A User’s Manual for DELSOL3”, Sandia National Laboratories, (1986)
16. Renewable Energy Technologies: Cost Analysis Series CSP, IRENA (2012), page 35
17. OECD <https://data.oecd.org/price/inflation-cpi.htm#indicator-chart>
18. IRENA, “Renewable Energy Generation Costs in 2014” (2015), page 104
19. G. Leyland, “Multi-Objective Optimisation Applied to Industrial Energy Problems” Ph.D. thesis, Energy Systems, Swiss Federal Technology Institute, Lausanne, Switzerland (2002)